HAL open science

Time domain modelling of room acoustics

Yiu Wai Lam, Jonathan Hargreaves

To cite this version:

Yiu Wai Lam, Jonathan Hargreaves. Time domain modelling of room acoustics. Acoustics 2012, Apr 2012, Nantes, France. hal-00811383

HAL Id: hal-00811383

https://hal.science/hal-00811383v1

Submitted on 23 Apr 2012

HAL is a multi-disciplinary open access archive for the deposit and dissemination of scientific research documents, whether they are published or not. The documents may come from teaching and research institutions in France or abroad, or from public or private research centers.

L'archive ouverte pluridisciplinaire **HAL**, est destinée au dépôt et à la diffusion de documents scientifiques de niveau recherche, publiés ou non, émanant des établissements d'enseignement et de recherche français ou étrangers, des laboratoires publics ou privés.

Time domain modelling of room acoustics

Y.W. Lam and J. Hargreaves

University of Salford, School of Computing, Science and Engineering, M5 4WT Salford, UK
y.w.lam@salford.ac.uk

Time domain modelling offers many advantages for room acoustics investigations. It directly generates the room's impulse response which is an important piece of information for acoustic quality assessment. It is efficient for broadband calculations over a short time duration. The most common room acoustics modelling method is currently based on geometrical room acoustics in the time domain. It is efficient and provides practical approximations. However, its accuracy is ultimately limited by its approximation of wave behaviours. Wave based models, which are more accurate but expensive, have been gaining interests due to more efficient numerical schemes. One example is the finite difference time domain method. This paper gives some examples of developments in this method for room acoustics. Another example is the time domain boundary element method. Although it is harder to implement, it has an advantage that a change in source or room does not require complete recalculation of the interaction matrix. This is useful for time variant simulation or auralisation. Here we also introduces the concept of 'wave matching', and see if it has the potential to be developed into a new, efficient time domain wave based modelling method.

1 Introduction

Sound naturally occurs in the time domain. In room acoustics the key feature that determines the acoustic quality is the room impulse response, which is a time domain feature. Time domain modelling should therefore be a more logical way to study room acoustics than conventional frequency domain methods. The room impulse response is also the pre-requisite for post-processing such as auralisation, which has become a common tool for architectural acoustics design in practice. Compared with frequency domain method, time domain modelling allows a one-pass broadband calculation. It can be said that time domain methods offer a distinct advantage in room acoustics design, and in fact in many other areas that involve interaction of waves with objects. Current commercial room acoustic simulation software almost exclusively approximates the propagation of sound geometrically - early reflections are typically evaluated deterministically using a variant of the ray tracing/image source method, which operates in the time domain. It is however somewhat ironic that results from these models are often presented in the frequency domain, in terms of room acoustic parameters in difference octave frequency bands. Part of the reason is that these models mostly trace the energy arrivals at the receiver, thus creating a histogram of reflections, rather than the true impulse response. Ignoring wave effects allows efficient computation algorithms at the expense of accuracy.

The application of energy-based geometric modelling to large space acoustics is well established nowadays. Its accuracy has been tested through a series of international round robin tests, e.g. [1, 2], and it has been accepted by many architectural consultants as a design tool. Over the last 2 decades, many improvements have been made to allow it to handle certain wave effects. Scattering coefficients and diffuse reflection algorithms were introduced to approximate non-specular reflections [3]. Diffraction can also be supported by implementing wedge diffraction formula [e.g. 4] or stochastic scattering of rays next to diffraction edges [5], although these often result in a substantial increase in computation costs as multiple order of diffraction are simulated. It is also possible to include phase information in the ray tracing processing or in the image method [6] to allow for wave interference effect to be modelled, but the extent that this can approximate complex boundary conditions is still not tested in realistic room conditions.

Methods that directly model wave effects, such as boundary element and finite element methods, offer better accuracy, especially at lower frequencies or in smaller rooms, at the expense of computational cost. These methods are traditionally applied in the frequency domain. One key reason for this is that the problem is much easier to formulate by breaking down the sound field and the boundary condition into their frequency components. The frequency domain boundary condition in particular is much more established than its time domain equivalent. It could be argued that a time domain solution is only an inverse Fourier Transform away from a frequency domain solution. However this will not be an efficient process if only the early part of the impulse response is needed. In such cases a direct time domain solution will be desirable. This paper will look at some of the popular time domain modelling methods, namely the finite difference time domain method and the time domain boundary element method, and introduces the new concept of 'wave matching', which aims to bridge the gap between wave and geometric models.

2 Finite Difference Time Domain Method

In recent years, the finite difference time domain (FDTD) method has become a popular wave based time domain method in room acoustics. A significant advantage of the method is that the basic FDTD equations for acoustics, whether they are based on the first order Euler and continuity equations or the single second order wave equation, are fairly straightforward and easy to implement, and therefore allow a model to be quickly established. The calculation can also be easily accelerated via parallelization such as through the use of GPGPU. However, there are several aspects that required improvements for the method to become practical for room acoustic simulation. The modelling of frequency dependent boundary conditions, the control of dispersion errors, and the implementation of sources are among the main issues of concern in the current development of the FDTD method in the acoustic field. The dispersion error, which appears as the spherical wave is propagated through a rectangular grid, needs to be suppressed by either a very fine mesh, with tens of sampling points per wavelength (e.g. 20 per λ) at the highest frequency of interest, or by a high order interpolation scheme. This raises the computation cost, although this can be somewhat offset by GPGPU

acceleration. Among the other issues, the ability to handle frequency dependent boundary impedance on irregular boundary geometry is fundamental to room acoustics applications. Also, the problem of source excitation has not received much attention compared to others, although the implementation of the source has a significant impact on the time response produced by the simulation particularly in room acoustics. In here, we will look at some recent developments in these two areas.

2.1 Simple transparent source

In FDTD simulation, being in the time domain, an excitation pulse can simply be assigned to a pressure node where the source should be. In terms of implementation, there are different implementation methods that are referred to by terms that are also frequently used in electromagnetic field - "hard", "soft" and "transparent" sources. In particular, a "transparent" source is seen as the best option for determining the system response to a pre-defined excitation without suffering from numerical artefacts created by other source types. However, a transparent source implementation requires knowledge of the grid impulse response, which has to be pre-calculated. In a room with boundaries, the grid response requires a very large computational domain to avoid reflections from the boundaries from interfering with the source node. It is therefore rather impractical due to the long calculation time required.

In a soft source implementation, the driving function is simply superimposed on the source node's normal response due to the FDTD update equations. However, the added changes give rise to a pressure function at the source node that is different from the intended excitation. It is therefore necessary in such an implementation to 'measure' the response at the source node, and use that to normalise the results at other nodes. This may be why soft source excitation has not seen much use in existing acoustics literature.

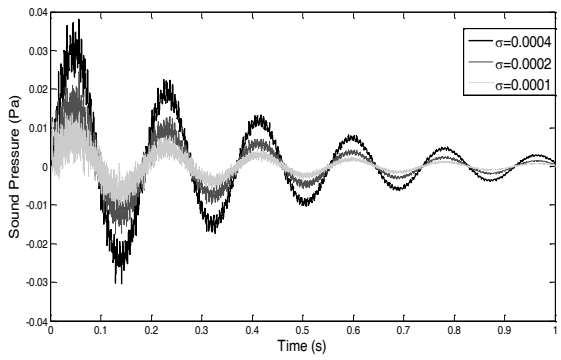

Figure 1 Time response in a rectangular room calculated by FDTD method using a Gaussian pulse with different pulse widths and a hard source implementation.

The simplest way to excite a FDTD grid is to impose a prescribed driving function on the source node. This source implementation is known as the hard source implementation, as the source node is not affected by the surrounding fluid (or nodes). Unfortunately, when the source is implemented in this way, an abrupt change is created between the update equations used by the source node and the surrounding nodes that could give rise to massive artifacts in the numerical results [7]. Fig.1 shows an example of such an artifact created by a hard source. The low frequency modulation seen in the time response is caused by holding the source node at zero after the initial Gaussian pulse, which caused in a build up of net overpressure that oscillates within the grid.

Obviously, it will be desirable to construct a source implementation that has the characteristic of a transparent source but has the simplicity of a hard or soft source. In Ref.[7], it was shown that such a construction is possible by a suitable choice of the source pulse, and allow the source node to revert from a hard source node to a soft source node after the main pulse has ended.

Since the occurrence of the low frequency modulation is linked to the lack of rarefaction at the end of the Gaussian pulse, the first logical step to take to eliminate the problem is to use a more realistic pulse shape. In this context a sine modulated Gaussian pulse, $g_s(t)$, is a suitable choice.

$$g_s(t) = -Ae^{-\frac{(t-t_0)^2}{2\sigma^2}} \cdot \sin\left(\omega_0(t-t_0)\right)$$

Using this pulse in a hard source implementation eliminates a large part of the low frequency modulation seen in Fig.1. However, some errors still persists, because the source node is still held at zero after the main pulse has ended, rather than following the normal FDTD update wave equations as in the surrounding nodes. A further step to remedy this is therefore taken to allow the source node to follow the update equation a short time after the main pulse, essentially reseting the source from a hard source to a soft source. This is termed a "time limited sine modulated Gauusian hard source" (TLSGH) in Ref.[7]. As long as the time limit is set after the main pulse has ended, the transit does not cause significant errors and the source appears as a true transparent source. Fig.2 shows the frequency response corresponding to Fig.1 but with this TLSGH implementation, with the time limit set at times when the pulse has decayed to less than 0.03% of its peak value. The FDTD results are compared with that calculated by the frequency domain boundary element method, which does not have the source implementation problem. Clearly the low frequency error has completely disappeared. In another word, the pulse response and frequency spectrum produced by the TLSGH are exactly those created by a true transparent source with the same pulse shape. At the same time, the TLSGH has the same computation efficiency as simple hard and soft source implementations.

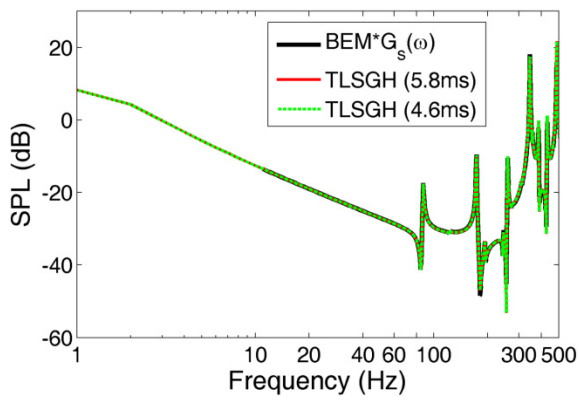

Figure 2 Frequency response at receiver of Fig.1 but calculated by the TLSGH source technique in FDTD, compared with BEM.

2.2 Frequency dependent boundary condition on irregular surfaces

The modelling of the interaction of sound wave with a boundary is a more challenging subject in the time domain than in the frequency domain. To implement proper boundary conditions in a time domain method, we first require a representation of the acoustical property of common wall surfaces, which is commonly defined in terms of impedance, reflection coefficient or absorption coefficient. Since most of these quantities are defined or measured in the frequency domain, we will need to determine how to transform these data into the time domain. This needs to be done carefully, since it has been shown that not all frequency domain surface impedance models are causal. In theory, the boundary condition can be presented as an impulse response to be convoluted with the FDTD update equations. Unfortunately, this is a rather time consuming process, especially so considering the large number of reflections involved in room acoustics.

There are various approximations [8-10] that can be used to speed up the calculation. For frequency dependent boundary condition, the impedance Z_B, as a function of the angular frequency ω, needs to be represented by a suitable rational function to ensure causality and stability. A convenient means of achieving this is to derive an approximation using a multi-degree-of-freedom (DOF) mechanical system representation. For low to mid frequency calculations, up to about 500Hz, a 2 DOF system proves to be effective for common fibrous type materials. Once approximated, the impedance condition equation can be transformed into the Z-domain using bilinear transform, and then incorporated into the FDTD scheme.

While the implementation of frequency dependent boundary conditions has received much attention in FDTD modeling, the problem of irregular boundary geometry has not received as much attention. If the boundary geometry does not fit into the regular mesh grid used for the FDTD calculation, a straightforward standard approach is to approximate the boundary using stepwise, stair-step type edges/patches that fit the mesh grid. For boundary conditions that are hard, the error appears to decrease significantly when nominally 40 points per wavelength is used [11]. However, for absorptive conditions that have large phase changes, the error in stair-step approximation could remain significant even at high grid resolutions. In addition, the existence of multiple reflections off the surface in a room acoustics setting may also compound the error. There is, however, no published work analyzing the accuracy of this stair-step approach for room acoustic simulations.

A more accurate means of dealing with arbitrary geometry is to use a conformal algorithm. A locally conformal technique that was used for electromagnetic FDTD modelling has been adopted for rigid surfaces in acoustics FDTD simulation [11]. Here, this approach is extended to include frequency dependent impedance surface, and will be used to analyze the error due to a stair-step approximation in a room acoustics setting.

The basic conformal formulation can be developed from an integral equation formulation. By integrating the acoustics governing differential equation over a volume V, which is bounded by a surface S, and then using the divergence theorem, one obtains,

$$\frac{\partial}{\partial t}\iiint_V p dV = -\rho_0 c^2 \iiint_V \nabla\cdot\mathbf{v} dV = -\rho_0 c^2 \oiint_S \mathbf{v}\cdot n dS$$

The integration can be applied to a cell in the FDTD that is intersected by an arbitrary boundary. Fig.3 shows a nominal intersected cell. It is assumed that the pressure node at (i,j,k) in the figure is located at the centre of the undistorted cell, and the pressure is constant over the entire volume of the cell, regardless of whether the centre is inside or outside the intersecting boundary.

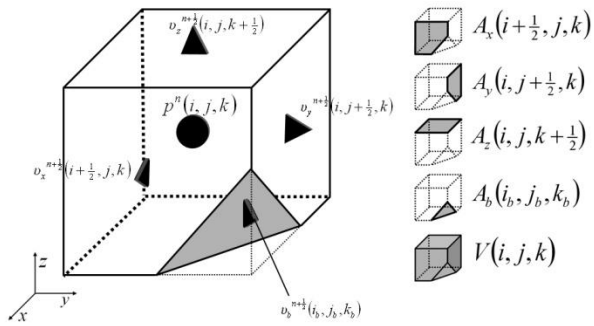

Figure 3 A nominal rectangular FDTD grid cell intersected by an arbitrary boundary.

Carrying out this integration within the cell results in an appropriate equation in FDTD format. The area A_b and the normal velocity υ_b are associated with the boundary impedance. For frequency dependent boundaries, υ_b can be calculated with the impedance formulated as a Z-domain filter.

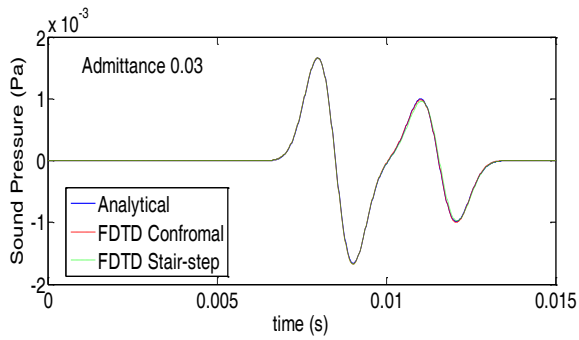

Figure 4 FDTD predictions against analytical solution of pulse reflection from a single inclined plane with constant admittance of 0.03.

The case of reflection from a simple inclined plane surface is used to test the accuracy of the conformal mapping method against the standard stair-step approximation. The inclination is about 26° from the horizontal. The source and receiver are arranged to give an incident angle of about 50°. The rectangular FDTD grid is deliberately aligned with the horizontal and the vertical, so that the inclined surface is approximated by either stair-steps or conformal mapping. About 34 points per wavelength at the upper frequency limit of 500 Hz is used in the stair-step approximation, which has been found to be sufficient for rigid surfaces in published literature. The surface impedance is assumed to be frequency independent, so that the analytical solution from Ref.[12] can be used to test the accuracy of the FDTD calculations. The first case

uses a reflective condition, with the surface admittance equals to 0.03. The result is shown in Fig.4. As expected, both FDTD approximations give good agreement with the analytical solution.

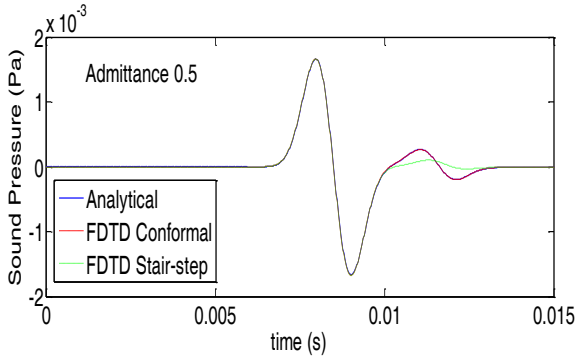

Figure 5 FDTD predictions against analytical solution of pulse reflection from a single inclined plane with constant admittance of 0.5.

A second test is done with a soft surface condition, with the admittance raised to 0.5. The result is shown in Fig.5. With a soft surface, the error of the stair-step approximation becomes apparent, while the conformal mapping maintains excellent agreement with the analytical solution. Further testing suggests that the error from the stair-step approximation tends to increase with softer surface, and at larger (more near glazing) incident angles.

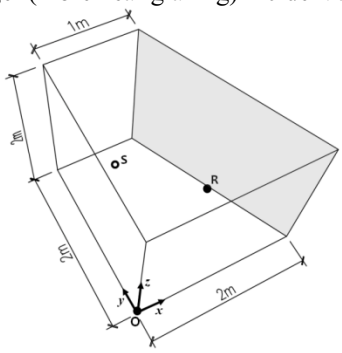

Figure 6 Test room with a tilted boundary that has a frequency dependent impedance.

In order to analyze the effect of the stair-step approximation in modeling room acoustics, a simple room with a tilted boundary is used, see Fig.6. The spatial resolution again gives about 34 points per wavelength at 500Hz. The TLSGH source implemented was used for the calculations. To simplify the comparison of the results, only the tilted boundary had a frequency dependent impedance. All other wall surfaces were fairly hard, with a constant admittance of 0.004. The frequency dependent impedance on the tilted boundary was simulated as rigidly backed fibrous material. The flow resistivity, σ, and the depth of the material were varied to give different absorptive properties. Figure 6 shows the calculated results for a fairly soft setting, with σ=32k Pa/m2 and depth=100mm. The magnitude of the reflection coefficient from this boundary drops slowly to about 0.5 at the highest frequency tested, 500Hz, with the phase change remains within about 20°. The legend 'NI-2DOF-I' corresponds to the 2DOF formulation for the impedance, while 'NRC-MP-I' corresponds to an approximate impedance obtained from augmenting an equivalent absorption coefficient with a minimum phase to simulate practical cases where only absorption coefficient rather than impedance is known. The text 'standard' refers to calculation using standard stair-step approximation. All are compared with the result from a boundary element calculation. Even with just one absorptive surface in the room, the stair-step approximation shows significant errors throughout the entire frequency range.

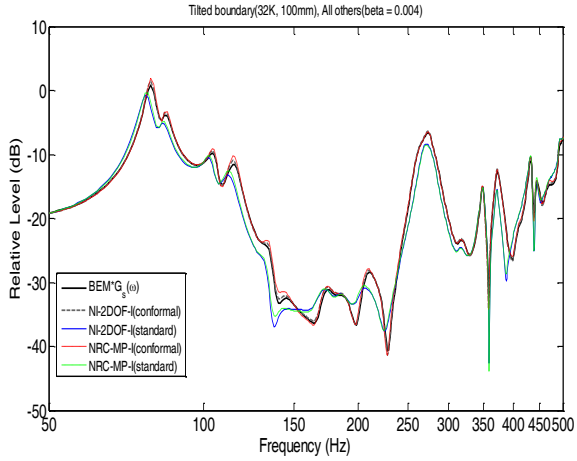

Figure 7 Comparison of FDTD calculated frequency responses with an absorptive titled boundary against BEM.

These test cases clearly show that using conformal mapping for complex boundary conditions in FDTD modelling has very good accuracy – comparable to that produced by the BEM. It is far more accurate than the stair-step approximations, which becomes more inaccurate when the boundary becomes more absorptive.

For FDTD calculations, we have shown that a simple formulation, namely the TLSGH, can be used to produce transparent source characteristics, and that stair-step approximation should not be used to model absorptive irregular boundaries. Instead a conformal mapping method shows excellent accuracy in all test cases. The combination of TLSGH and conformal mapping should make FDTD a lot more applicable to room acoustics calculations. However, FDTD calculation remains time consuming because of the high grid and time step resolution required to suppress dispersion errors. GPGPU acceleration would help to reduce computational cost, but it would still be very expensive relative to standard geometrical models. The conformal mapping approach also requires intrigue handling of geometry. Hence it is still necessary to look at alternative time domain modelling techniques.

3 The Boundary Element Method

The Boundary Element Method (BEM) has been studied in detail by the acoustics research group at Salford for nearly twenty years. It has the advantage of requiring fewer degrees of freedom than volumetric methods such as FDTD, since it only requires the boundary between the air and obstacle to be modelled, and this reduced dimensionality has the potential to provide substantial cost savings for large and/or high frequency problems. Schemes for efficiently representing and evaluating these highly oscillatory problems are attracting substantial research interest [13] and the dense interaction matrices may be compressed using the Fast Multipole Method.

Most BEMs assume time-harmonic excitation but this assumption may be dropped leading to the time domain BEM. This approach was first published in 1962 but computational cost and stability issues plagued the method and only in the last decade or so has the rate of progress increased and commercial implementations appeared. In particular the following have been implemented: the Combined Field Integral Equation (CFIE) [14], being the time domain equivalent of the Burton and Miller formulation to addresses the non-uniqueness of the complementary interior problem; Fast Multipole style acceleration [15]; Galerkin schemes, which have been proven to have unconditional stability [16,17]; Convolution Quadrature method [18], which offers both a rigorous mathematical analysis and excellent computational cost scaling. At Salford we have focussed upon the more practical aspects of transferring some of our frequency domain models of acoustic treatments to the time domain. This has required development of representations of: bodies with welled sections, using a delayed reflection boundary condition [19]; bodies which comprise both thick sections and thin fins [20]; bodies with arbitrary frequency dependent surface impedance, using digital reflectance filters [21].

In summary it can be seen that although FDTD is currently the dominant time domain wave method in use in computational room acoustics, BEM research is very active and the advances being made, particularly in the applied maths field, may well allow the time domain BEM to finally mature and become widely used in acoustic simulation.

4 Introducing 'Wave Matching'

This section of the paper describes a prototype time domain BEM formulation which we are calling 'Wave Matching'. In essence this aims to reflect how we think of acoustic scattering; as a sum of geometrically reflected and diffracted components with the former being dominant at high frequencies. We believe time domain BEM a good place to start in a search to unify wave and geometric approaches since both classes of algorithm work with surface geometry and analytically compute how elementary sound sources propagate through the media unobstructed, so the problem is one of computing the reflections and scattering from obstacles. The main difference between the algorithms is that BEM attacks the problem by numerical discretisation of the total field whereas geometric methods trace reflections individually according to a high-frequency asymptotic approximation.

Ideally we would like to retain the positive characteristics of both algorithms. Geometric methods are efficient because they trace a relatively small number of sound propagation paths; this is equivalent to seeking great sparsity in BEM interaction matrices. However they offer no way to re-unite sound energy arriving at a surface from different propagation paths, so suffer from an exponential increase in the number of propagation paths with each order of reflection; this is particularly severe when edge diffraction terms are included [4]. Time domain BEM in contrast uses a constant number of degrees of freedom versus time and any sound wave arriving at the surface is mapped onto a weighted sum of interpolating functions.

In the following sections we will show that, given appropriate interpolation functions, the scattering integral over a surface which is large with respect to wavelength may be stated as a geometric term plus a diffracted term involving only a 1D edge integral. Then we will examine a Gallerkin testing integral, discuss its motivation, interpretation and how it might be evaluated efficiently with the proposed interpolation scheme, and finally show results that suggest that doing so produces interaction matrices with a very small number of significant coefficients. Despite the fact that this paper concerns developments in time domain modelling many of the statements which follow will be given in the frequency domain. This is because the frequency domain BEM formulation is more succinct and familiar to a wider audience, plus the numerical test case was implemented using harmonic functions. How the algorithm might be implemented in the time domain is outlined alongside.

4.1 Choice of interpolating functions

A BEM to model scattering of sound by an obstacle has three distinct phases depicted in Figure 8. First the incident sound φ_i arriving the obstacle from the sources is calculated, then the total sound φ_t at the surface of the object is solved for by considering the mutual interactions between parts of the obstacle, and finally the scattered sound φ_s at any receivers is calculated from this total surface sound. The total sound on the surface is approximated by a weighted sum of a set of interpolation functions $f_m(\mathbf{y})$ and the primary objective is to solve for the set of weights φ_m:

$$\varphi_t(\mathbf{y}) = \sum_m \varphi_m f_m(\mathbf{y})$$

In most BEM formulations the surface is partitioned into elements which are small with respect to wavelength and only a small number of interpolation functions will be non-zero on each element. Each interpolation function has an associated testing function $f_m^*(\mathbf{x})$ used to evaluate what component of the incoming sound should be mapped onto its coefficient; in a Galerkin scheme these are typically the adjoints of the interpolation functions and in a collocation scheme they are delta functions located at the collocation points. In both cases the objective is to achieve a scheme where the function pairs are orthogonal over the surface S:

$$\iint_S f_m(\mathbf{x}) f_n^*(\mathbf{x}) d\mathbf{x} = 0 \text{ if } m \neq n$$

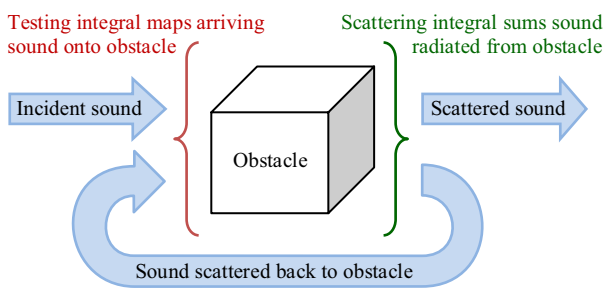

Figure 8 Solution process in a BEM model

There are however other families of orthogonal functions which could satisfy this criteria. One option which has attracted attention for the frequency domain BEM is the use of oscillatory interpolation functions [22,23], since these might be able to capture some of the behaviour of the solution allowing larger elements for the same accuracy. However because the oscillatory functions are multiplied by polynomial interpolators it is unclear how the integral transform described in the next section might be applied, so in this test case we instead apply a 2D Fourier series decomposition to the sound on each face of the obstacle. The interpolation functions are easiest to state if four summation indices are used:

$$\varphi_t(\mathbf{y}) = \sum_a \sum_m \sum_n \sum_\kappa \varphi_{a,m,n,\kappa} f_{a,m,n,\kappa}(\mathbf{y})$$

$$f_{a,m,n,\kappa}(\mathbf{y}) = \begin{cases} e^{i[\mathbf{y}-\mathbf{v}_a]\cdot\mathbf{k}_{a,m,n,\kappa}} & \text{if } \mathbf{y} \in S_a \\ 0 & \text{otherwise} \end{cases}$$

Here the a refers to the ath face S_a, defined by a corner vertex $\mathbf{v}_a$ and two perpendicular edge vectors $\mathbf{e}_{a;1}$ and $\mathbf{e}_{a;2}$. m and n are the indices of the Fourier Series on the surface, so may take any integer value, and $\kappa = \pm 1$. The surface normal unit vector $\hat{\mathbf{n}}_a$ is uniform over S_a and points into the medium. The wave direction vectors $\mathbf{k}_{a,m,n,\kappa}$ are given by:

$$\mathbf{k}_{a;m,n,\kappa} = \frac{2\pi m}{|\mathbf{e}_{a;1}|}\hat{\mathbf{e}}_{y;1} + \frac{2\pi n}{|\mathbf{e}_{a;2}|}\hat{\mathbf{e}}_{y;2} + \kappa\hat{\mathbf{n}}_a\sqrt{k^2 - \left(2\pi m/|\mathbf{e}_{a;1}|\right)^2 - \left(2\pi n/|\mathbf{e}_{a;2}|\right)^2}$$

The first two terms of the wave vectors define the Fourier series decomposition over S_a. The right-most term is zero on S_a (since $[\mathbf{y}-\mathbf{v}_a]\cdot\hat{\mathbf{n}}_a = 0$ if $\mathbf{y} \in S_a$) and exists for the purpose of making the interpolation function satisfy the wave equation; the motivation for this will become apparent in the next section. The wave vectors therefore define a family of propagating plane waves in the medium, commonly known as a wavenumber spectrum, and the interpolation functions are snapshots through them on the surface hence can capture oscillations at wavelengths which at first do not appear to match the wavelength in air (see inset). The term κ is necessary to distinguish between the two possible waves which may cause the same surface pressure; one with $\kappa = 1$ travelling out of the obstacle and one with $\kappa = -1$ travelling in to the obstacle. It is worth noting that for large magnitudes of m and n the term inside the square root may become negative and the surface normal component of $\mathbf{k}$ become imaginary; these are evanescent wave terms and valid parts of the solution.

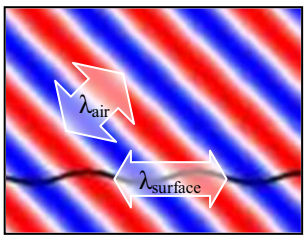

The physical interpretation of the above scheme as a family of travelling plane waves makes it easy to imagine a time domain equivalent, where the variation of the waves with time and/or propagation direction is no longer strictly harmonic and phase lag manifests as delay hence $e^{i[\mathbf{y}-\mathbf{v}_a]\cdot\mathbf{k}_{a,m,n,\kappa}}$ is replaced by $f\left(t - [\mathbf{y}-\mathbf{v}_a]\cdot\mathbf{k}_{a,m,n,\kappa}/c\right)$, where f is some arbitrary interpolating function in time. The Fourier series decomposition over the surface works neatly because the frequency domain formulation implies that a Fourier decomposition has already been applied in time. To create a transient version of the scheme we would therefore look to a system of non-periodic orthogonal basis, such as wavelets, and apply those to both space and time in an equivalent manner.

4.2 Efficient computation of scattering

The scattering integral evaluates the scattered sound φ_s at location $\mathbf{x}$ due to the total sound distribution φ_t on S and is used to evaluate the sound scattered from the obstacle both to receivers and back to the obstacle itself. It is given here in the frequency domain but the time domain statement is identical except that φ and G are time variant and the multiplications between them are replaced by convolutions:

$$\varphi_s(\mathbf{x}) = \iint_S \left[\varphi_t \frac{\partial G}{\partial n_y} - G\frac{\partial \varphi_t}{\partial n_y}\right] d\mathbf{y}$$

$G(\mathbf{x},\mathbf{y})$ is the free space Green's function which describes how sound travels from a point source at $\mathbf{y}$ to an observer at $\mathbf{x}$ and intuitively comprises a propagation delay and a reduction in magnitude with distance $R = |\mathbf{x}-\mathbf{y}|$. In the frequency domain this is written as a phase lag, so $G(\mathbf{x},\mathbf{y}) = e^{ikR}/4\pi R$, where we've assumed all quantities vary with $e^{-i\omega t}$, and in the time domain it appears as a retarded delta function so $G(\mathbf{x},\mathbf{y}) = \delta(t - R/c)/4\pi R$. Sound is given as velocity potential φ, a non-physical quantity but one which is useful as pressure and particle velocity may be found from it by $p = -\rho\dot{\varphi}$ and $\mathbf{v} = \nabla\varphi$. The operator $\partial/\partial n_y \equiv \hat{\mathbf{n}}_\mathbf{y}\cdot\nabla_\mathbf{y}$ denotes the component of the gradient in the direction of the surface normal vector at $\mathbf{y}$ and is often called the surface normal derivative.

It is well know that when using planar elements and piece-wise constant spatial interpolation functions the scattering integral may be transformed to a contour integral around the edge of each element plus a singularity term [24-26] allowing efficient evaluation. It appears to be less well known that this is just the $m = n = 0$ term in the interpolation scheme above and every term in the scheme may be integrated in this way [27]:

$$\iint_S \left[f_{a,m,n,\kappa}\frac{\partial G}{\partial n_y} - G\frac{\partial f_{a,m,n,\kappa}}{\partial n_y}\right] d\mathbf{y} = \text{illum}_{S_a,\mathbf{k}_{a,m,n,\kappa}}(\mathbf{x})e^{i[\mathbf{x}-\mathbf{v}_a]\cdot\mathbf{k}_{a,m,n,\kappa}} + \oint_{S_a} f_{a,m,n,\kappa}G\frac{\mathbf{k}_{a,m,n,\kappa}\times\mathbf{R}}{Rk - \mathbf{R}\cdot\mathbf{k}_{a,m,n,\kappa}}\cdot d\boldsymbol{l}_\mathbf{y}$$

Here $\mathbf{R} = \mathbf{x}-\mathbf{y}$ and $\text{illum}_{S_a,\mathbf{k}_{a,m,n,\kappa}}(\mathbf{x}) = \kappa$ if a line starting from the observation point $\mathbf{x}$ and pointing in the direction $-\mathbf{k}_{a,m,n,\kappa}$ passes through S_a, otherwise it is zero; this describes the geometric propagation zone of $f_{a,m,n,\kappa}$. The contour integrand contains the interpolation function, the Green's function to the receiver and a term which may be thought of as an 'edge-directivity' and describes the diffracted wave. Once again the time domain statement is identical except that the plane wave term and Green's function are replaced by their time domain equivalents and multiplication becomes convolution. The integration process is efficient, particularly for high frequency waves, compared to 2D surface integration since the geometric term can be evaluated analytically and the diffracted term requires only a 1D edge integral to be evaluated.

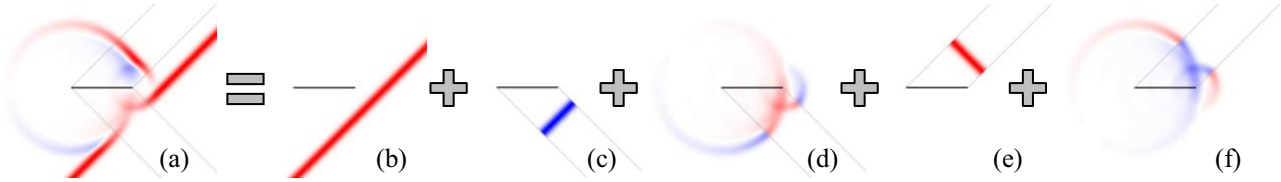

Figure 9: First order scattering by a square plate illuminated by a plane wave at 45°: a) Total; b) Incident; c) Shadow (geometric); d) Shadow (diffraction); e) Reflection (geometric); f) Reflection (diffraction).

As is often the case, visualisation in the time domain makes the process easier to understand so this is depicted in Figure 9 for scattering by a thin square plate. First the incident wave (b) is mapped onto an incoming wave and it scatters into the medium behind the surface section causing the necessary shadow effect (c,d). The incoming wave term is then coupled to a matching outgoing term (e,f) by a frequency and angle dependent reflectance function (as in [21]) giving a reflected wave whose spectral content has been modified according to the surface impedance of the scattering object. The next challenge is to efficiently match an arbitrary incident wave onto a family of interpolation wave functions; this will be discussed in the next section.

4.3 The 'wave matching' testing integral

Because the interpolating functions overlap with one another collocation testing is not appropriate and Galerkin testing integrals must be evaluated over the entire surface section. Here we follow the ideas presented in 16 and 17.

The instantaneous energy of an acoustic wave is:

$$E = \frac{\rho}{2}\left[|\mathbf{v}|^2 + \frac{|p|^2}{\rho^2 \mathrm{c}^2}\right] = \frac{\rho}{2}\left[|\nabla\varphi|^2 + \frac{|\dot{\varphi}|^2}{\mathrm{c}^2}\right]$$

Because our test case uses complex-valued harmonic functions we must be careful to respect the modulus operators and use complex conjugates:

$$E = \frac{\rho}{2}\left[\nabla\varphi \cdot \overline{\nabla\varphi} + \frac{\dot{\varphi}}{\mathrm{c}}\frac{\overline{\dot{\varphi}}}{\mathrm{c}}\right]$$

Acoustic power flux is more commonly known as acoustic intensity:

$$\mathbf{I} = p\mathbf{v} = -\frac{\rho}{2}\left[\dot{\varphi}\overline{\nabla\varphi} + \overline{\dot{\varphi}}\nabla\varphi\right]$$

Since φ and ψ satisfy the wave equation they are related by the Energy flux relation $\dot{E} = -\nabla \cdot \mathbf{I}$ so the divergence theorem may be applied:

$$\iiint_V \dot{E}\, dV = -\iint_{S=\partial V} \hat{\mathbf{n}}_{\mathbf{x}} \cdot \mathbf{I}\, d\mathbf{x}$$

Ultimately the aim is to integrate this with respect to time and define an energy norm over V (as is done in 16 and 17), but since our test case is in the frequency domain we may simply use the fact that energy is constant versus time hence $\dot{E} = 0$ and by substitution:

$$\iint_S \left[\dot{\varphi}\frac{\overline{\partial\varphi}}{\partial n_x} + \overline{\dot{\varphi}}\frac{\partial\varphi}{\partial n_x}\right] d\mathbf{x} = 0$$

Noting that φ has $e^{-i\omega t}$ time dependence whereas $\overline{\varphi}$ has $e^{i\omega t}$ so we have:

$$\iint_S \left[\varphi\frac{\overline{\partial\varphi}}{\partial n_x} - \overline{\varphi}\frac{\partial\varphi}{\partial n_x}\right] d\mathbf{x} = 0$$

The similarity of this statement to the scattering integral is quite striking; if $\overline{\varphi}$ is replaced by G then the integrals are identical. The suggests an interesting interpretation of the scattering integral, that instead of representing a sum of monopole and dipole sources on S it is instead measuring the common energy between the wave φ and a convergent spherical wave $e^{-ikR}/4\pi R$ which coalesces at $\mathbf{x}$. $\varphi_s(\mathbf{x})$ 'pops out' because the divergence theorem cannot be applied at $\mathbf{x}$ since G is singular when $\mathbf{y} = \mathbf{x}$. Crucially this similarity also suggests that it might also be possible to evaluate the testing integral using Stokes theorem, since the primary requirement for it to be applied was that the waves involved both satisfy the wave equation, which φ and $\overline{\varphi}$ do. This would mean that the testing integral could also be evaluated as a 1D contour around the edge of the testing face, greatly reducing integration cost particularly for oscillatory integrands. It is also interesting to note that a boundary condition equivalent to the CFIE [14] arises if $\overline{\varphi}$ is replaced by $e^{ik\hat{\mathbf{n}}_{\mathbf{y}}\cdot\mathbf{x}}$, being the conjugate of a plane wave travelling into the obstacle.

To form a BEM scheme we will substitute each of the testing functions $f^*_{b,p,q,\xi}$ (which are the conjugates of the interpolation functions) into $\overline{\varphi}$ and use $\varphi = \varphi_i + \varphi_s$, where φ_s will be computed using the scattering integral. This result is the numerical scheme which may be readily solved by collapsing the indexes into a matrix equation:

$$\sum_a \sum_m \sum_n \sum_\kappa \mathrm{Z}_{a,m,n,\kappa,b,p,q,\xi}\varphi_{a,m,n,\kappa} = \mathrm{e}_{b,p,q,\xi}$$

$$\mathrm{e}_{b,p,q,\xi} = \iint_S \left[f^*_{b,p,q,\xi}\frac{\partial\varphi_i}{\partial n_x} - \varphi_i\frac{\partial f^*_{b,p,q,\xi}}{\partial n_x}\right] d\mathbf{x}$$

$$\begin{aligned}\mathrm{Z}_{a,m,n,\kappa,b,p,q,\xi} &= \iint_{S_b}\iint_{S_a}\left[f^*_{b,p,q,\xi} f_{a,m,n,\kappa}\frac{\partial^2}{\partial n_x \partial n_y}G\right.\\ &+ G\frac{\partial f^*_{b,p,q,\xi}}{\partial n_x}\frac{\partial f_{a,m,n,\kappa}}{\partial n_y}\\ &- f^*_{b,p,q,\xi}\frac{\partial f_{a,m,n,\kappa}}{\partial n_y}\frac{\partial G}{\partial n_x}\\ &\left.- f_{a,m,n,\kappa}\frac{\partial f^*_{b,p,q,\xi}}{\partial n_x}\frac{\partial G}{\partial n_y}\right] d\mathbf{y}\, d\mathbf{x}\end{aligned}$$

4.4 Interactions Coefficients

In what follows we consider evaluation of the Z coefficients for a test case scheme which uses planar rectangular surface sections. We are interested in whether the wave matching method will start to behave like a geometric method as the frequency is increased. Because the interpolation functions form a spatial Fourier series over the surface sections the double surface integral may be quickly evaluated using a four-dimensional FFT. We may also substitute the following relations where the scalar product terms are constant over the surface sections and may be brought outside the integrals:

$$\frac{\partial f_{a,m,n,\kappa}}{\partial n_y} = i\hat{\mathbf{n}}_\mathbf{y} \cdot \mathbf{k}_{a;m,n,\kappa} f_{a,m,n,\kappa}$$

$$\frac{\partial f^*_{b,p,q,\xi}}{\partial n_x} = -i\hat{\mathbf{n}}_\mathbf{x} \cdot \mathbf{k}_{b,p,q,\xi} f^*_{b,p,q,\xi}$$

Our test case is to evaluate the interactions between the interpolation functions on two 1m squared planar surface sections spaced 1m apart (see Figure 10). Their interaction was evaluated using both conventional piecewise-constant elements and the plane wave interpolation functions described above so that comparisons might be made. In both cases 32 elements or FFT nodes were used in each direction giving 32 × 32 × 2 = 2,048 degrees of freedom on each panel (the 2 is to account for the upward and downward wave directions) and $2{,}048^2$ = 4,194,304 interactions between them.

The histogram below shows the magnitudes of the interaction coefficients computed using elements (red) and the new wave matching scheme (green), each normalised in magnitude (horizontal axis) to their largest value, computed for $k = 8\pi$, so four oscillations in 1m. The main result here is that the magnitudes of the element interactions are all bunched around a similar range, so almost all of them are required to give an accurate representation of the interaction from S_a to S_b, whereas the vast majority of the wave matching interaction coefficients are over 100 times smaller than the largest. Figure 12 shows a zoomed in view of the bottom left of Figure 11 (without the element interactions) so the very small number of significant wave matching interactions can be seen. Only 106 interactions are larger than one tenth of the largest, and only 5806 are larger than one hundredth. Compared to the total number of interactions in the matrix (4,194,304) these are very small numbers. In contrast the element based discretisation has around 1,000,000 interactions larger than one tenth of the largest, and almost all are larger than one hundredth.

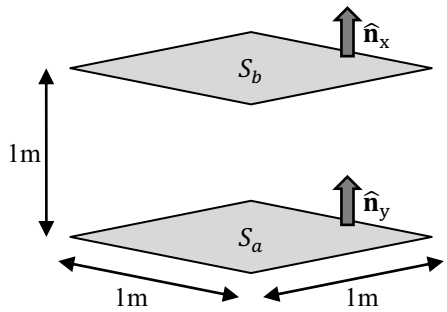

Figure 10: Numerical test case. Two 1m^2 parallel planar surface sections spaced 1m apart.

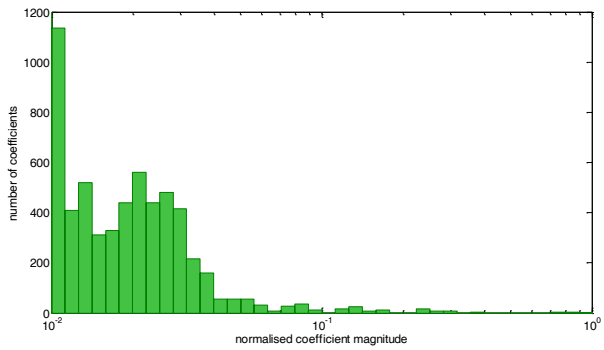

Figure 12: Zoom in on bottom right of Figure 11.

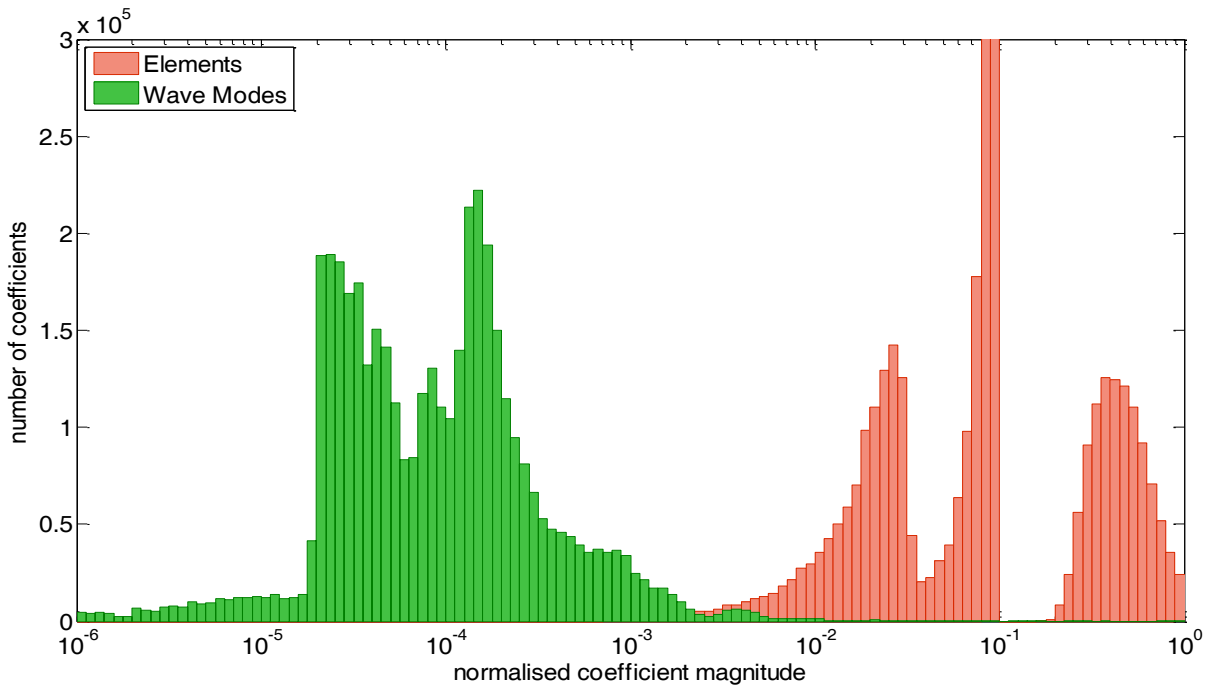

Figure 11: Histogram of the magnitude of interaction coefficients normalised to their larges value.

This is very positive result for the wave matching scheme. In addition the largest coefficients all satisfy $m = p$, $n = q$, and $\kappa = \xi = +1$, so the scheme has correctly matched the components that have a strong geometric similarity (κ and ξ must both be positive since the scheme is looking for waves travelling upwards from $S_a$to S_b). Ideally this characteristic will also mean that the number of significant interactions rises slowly with frequency, as the number of waves with a strong geometric overlap will remain small.

Figure 13 depicts this trend for the 'one tenth of largest' and 'one hundredth of largest' measures discussed above. It can be seen that the number of significant interactions does rise with frequency; a numerical fit shows this to be approximately with k^2. This is perhaps unsurprising since the wavenumber spectrum will become more densely spaced in angle as k increases, meaning more interpolation modes will geometrically radiate onto the other surface section. However it still performs vastly better than the standard k^4 interactions trend that conventional surface elements dictate, suggesting it would be much more suited to simulating high frequency scattering than standard BEM methods are.

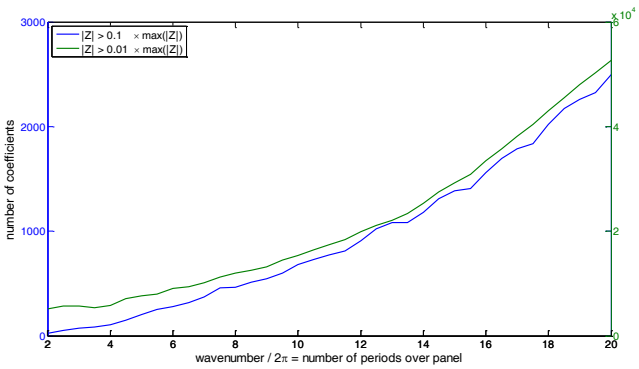

Figure 13: Number of significant interactions versus frequency

5 Conclusion

Here we have given an overview of time domain modelling for Room Acoustics, including the Finite Difference Time Domain method and a new variant of the time domain Boundary Element Method called 'Wave Matching'. As computation power continues to increase these are likely to gain further popularity as acoustic prediction tools.

References

[1] I. Bork, "A Comparison of Room Simulation Software - The 2nd Round Robin on Room Acoustical Computer Simulation", Acta Acustica 86: 943-956 (2000)

[2] I. Bork, "Simulation and measurement of auditorium acoustics - the round robins on room acoustical simulation", Proc. of the Inst. of Acous. 24 (2002)

[3] Y. W. Lam, "A comparison of three diffuse reflection modeling methods used in room acoustics computer models", J. Acous. Soc. Am. 100: 2181-2192 (1996)

[4] U P. T. Calamia, B. E. Markham and U. P.Svensson, "Diffraction Culling for Virtual-Acoustic Simulations", Acta Acustica 94 (6): 907-920 (2008)

[5] U. M. Stephenson, "An Energetic Approach for the Simulation of Diffraction within ray Tracing based on the Uncertainty Relation", ACUSTICA united with acta acustica, 96 (3): 516-535 (2010)

[6] Y. W. Lam, "Issues for Computer Modelling of Room Acoustics in Non-Concert Hall Settings", Acoust. Sci. & Tech. 26 (2): 145-155 (2005)

[7] H. Jeong and Y. W. Lam, "Source implementation to eliminate low-frequency artifacts in finite difference time domain room acoustic simulation", J. Acoust. Soc. Am. 131(1): 258–268 (2012)

[8] C. H. Lam, B. J. Kooij, and T. D. Hoop, "Impulsive sound reflection from an absorptive and dispersive planar boundary," J. Acoust. Soc. Am, 116: 677-685 (2004).

[9] K. Y. Fung and Xiaodong Jing, "Characterization of impedance boundary as damped harmonic oscillators via impulse reflection," J. Acoust. Soc. Am. 119: 3831-3838 (2006).

[10] S. Sakamoto, H. Nagamoto, A. Ushiyama and H. Tachibana, "Calculation of impulse responses and acoustic parameters in a hall by the finite-difference time-domain method," Acoustical science and technology. 29: 256-265 (2008).

[11] J. G. Tolan and J. B. Schneider, "Locally conformal method for acoustic finite-difference time-domain modeling of rigid surfaces," J. Acoust. Soc. Am. 114: 2575-2581 (2003)

[12] Martin Ochmann, "Closed form solutions for the acoustical impulse response over a masslike or an absorbing plane", J. Acoust. Soc. Am. 129 (6): 3502–3512 (2011)

[13] S. N. Chandler-Wilde, I. G. Graham, S. Langdon and E. A. Spence, "Numerical-asymptotic boundary integral methods in high frequency acoustic scattering" Acta Numerica (to appear)

[14] A. A. Ergin, B. Shanker and E. Michielssen, "Analysis of transient wave scattering from rigid bodies using a Burton-Miller approach", J. Acoust. Soc. Am. Vol. 106 (5): 2396-2404 (1999)

[15] A. A. Ergin, B. Shanker and E. Michielssen, "Fast analysis of transient acoustic wave scattering from rigid bodies using the multilevel plane wave time

domain algorithm", J. Acoust. Soc. Am. 107 (3): 1168-1178 (2000)

[16] T. Ha-Duong, B. Ludwig and I. Terrasse; "A Galerkin BEM for transient acoustic scattering by an absorbing obstacle" Int. J. Numer. Meth. Engng. 57: 1845–1882 (2003)

[17] A. Aimi, M. Diligenti, C. Guardasoni, I. Mazzieri and S. Panizzi; "An energy approach to space–time Galerkin BEM for wave propagation problems" Int. J. Numer. Meth. Engng. 80: 1196–1240 (2009)

[18] L. Banjai "Multistep and multistage convolution quadrature for the wave equation: Algorithms and experiments", SIAM J. Sci. Comput. 32(5): 2964-2994, (2010)

[19] J. A. Hargreaves and T. J. Cox, "A transient boundary element method model of Schroeder diffuser scattering using well mouth impedance", J.Acoust.Soc.Am. 124 (5): 2942-2951 (2008)

[20] J. A. Hargreaves and T. J. Cox, "A transient boundary element method for acoustic scattering from mixed regular and thin rigid bodies", Acta Acustica 95: 678-689 (2009)

[21] J. A. Hargreaves, "Simulating transient scattering from obstacles with frequency-dependent surface impedance", European Acoustics Association "Forum Acusticum" conference, Aalborg, July 2011

[22] E. Perrey-Debain, J. Trevelyan and P. Bettess, "Wave boundary elements: a theoretical overview presenting applications in scattering of short waves", Eng. Anal. Bound. Elem. 28(2): 131–141 (2004)

[23] H. Beriot, E. Perrey-Debain, M. BenTahar and C. Vayssade; "Plane wave basis in Galerkin BEM for bidimensional wave scattering", Eng. Anal. Bound. Elem. 34: 130–143 (2010)

[24] T. Terai, "On the calculation of fields around three-dimensional objects by integral equation method", J. Sound Vib. 69 (1): 71 – 100 (1980)

[25] Y. Kawai and T. Terai, "A Numerical Method for the Calculation of Transient Acoustic Scattering from Thin Rigid Plates", J. Sound Vib. 141 (1): 83 – 96 (1990)

[26] J. A. Hargreaves, "Time domain boundary element method for room acoustics", PhD thesis, University of Salford (2007) http://usir.salford.ac.uk/16604/

[27] K. Miyamoto and E. Wolf, "Generalization of the Maggi-Rubinowicz Theory of the Boundary Diffraction Wave – Part I", J. Opt. Soc. Am. 52 (6) 615-625 (1962)